PAPER Special Section on Wideband Systems

Filter-and-Forward-Based Full-Duplex Relaying in Frequency-Selective Channels

Shogo KOYANAGI[†], ***Student Member and*** **Teruyuki MIYAJIMA**[†a)], ***Member***

SUMMARY In this paper, we consider full-duplex (FD) relay networks with filter-and-forward (FF)-based multiple relays (FD-FF), where relay filters jointly mitigate self-interference (SI), inter-relay interference (IRI), and inter-symbol interference. We consider the filter design problem based on signal-to-noise-plus-interference ratio maximization subject to a total relay transmit power constraint. To make the problem tractable, we propose two methods: one that imposes an additional constraint whereby the filter responses to SI and IRI are nulled, and the other that makes i.i.d. assumptions on the relay transmit signals. Simulation results show that the proposed FD-FF scheme outperforms a conventional FF scheme in half-duplex mode. We also consider the filter design when only second-order statistics of channel path gains are available.

key words: *full-duplex, filter-and-forward, cooperative-relaying, inter-relay interference, second-order statistics*

1. Introduction

Full-duplex (FD) technology has recently attracted considerable interest because of its potential to increase network capacity in wireless communications [1], [2]. In FD mode, wireless devices can simultaneously transmit and receive in the same band and thus achieve twice the level of spectral efficiency compared to the traditional half-duplex (HD) mode. The primary technical challenge to obtaining the benefit mentioned above is to suppress self-interference (SI), whose reception power is 100 dB higher than that of interested signals from a transmitter [3]. A significant amount of SI can be suppressed in propagation [4] and analog-circuit [5] domains, but residual SI inevitably remains. To cope with the residual SI, digital-domain suppression is critical.

One suitable application of the FD mode is relay transmission [2]. FD relaying can expand radio coverage and improve network capacity without additional time and frequency resources. When common relaying protocols such as amplified-and-forward (AF) and decode-and-forward (DF) are employed, a conventional approach to mitigate SI at an FD relay node is to employ an interference canceller, which subtracts an SI replica from a corrupted received signal [6]–[9] but requires an additional cost to be implemented. Another issue is to combat inter-symbol interference (ISI) in frequency-selective channels. For this purpose, orthogonal-frequency division-multiplexing (OFDM) is commonly used in AF and DF relaying [8], [10]. However, OFDM is not suitable for power efficient wireless devices because its transmit signal has a high peak-to-average power ratio (PAPR) and its use of cyclic prefix (CP) results in a loss of bandwidth efficiency. In terms of PAPR and bandwidth efficiency, single-carrier transmission without CP is desirable. However, mitigating ISI in addition to SI is crucial.

Filter-and-forward (FF) relaying, which consists of relays equipped with an FIR filter, is very effective at reducing the effect of ISI [11], [12]. Combining the FF protocol with FD relaying in single-carrier transmission, we can expect that both SI and ISI are simultaneously suppressed by FIR filtering without an additional SI canceller. However, studies on combining FF and FD relaying are scarce. Only one study has considered the use of a feedback FIR filter to mitigate both SI and ISI at a MIMO relay [13]. However, an unrealistic amount of time is required to adapt the feedback filter blindly.

The use of multiple relay nodes obtains the requisite spatial diversity and improves system performance by cooperative beamforming (BF), which has been intensively developed for HD relaying [11], [12], [14]–[16]. The cooperative BF can be applied to various wireless systems such as mobile communication systems [15] and wireless sensor networks [16]. By contrast, if cooperative-BF is applied to FD relaying, using multiple FD relays causes not only SI but also inter-relay interference (IRI) [17]. Simultaneously mitigating SI and IRI is a challenge. To the best of our knowledge, no studies on FD systems equipped with cooperative-BF have been reported.

In this paper, we consider full-duplex relaying networks with multiple relay nodes based on the FF protocol over frequency-selective channels. Here, we need to jointly mitigate SI, IRI, and ISI, while achieving satisfactory performance by cooperative-relaying. We propose two methods for filter design based on signal-to-noise-plus-interference ratio (SINR) maximization at the destination, subject to a total relay transmit power constraint. For numerical results, we evaluate the performances of the proposed filter design methods and compare the proposed full-duplex-based FF (FD-FF) relaying scheme to a conventional HD-based FF scheme [11]. In addition, we apply the filter design to a partial channel state information case in which only second-order statistics (SOS) of relay-to-destination channel path gains are available.

In this paper, we use the following notations: $(\cdot)^T$, $(\cdot)^H$ indicate matrix or vector transpose and Hermitian transpose, respectively. The operator $\otimes$ denotes the Kronecker

Manuscript received April 4, 2018.
Manuscript revised August 22, 2018.

[†]The authors are with the Graduate School of Science and Engineering, Ibaraki University, Hitachi-shi, 316-8511 Japan.
a) E-mail: teruyuki.miyajima.spc@vc.ibaraki.ac.jp

DOI: 10.1587/transfun.E102.A.177

product. $\mathbf{0}_{N\times M}$ is an $N \times M$ matrix, all of whose elements are equal to zero, $\mathbf{I}_N$ denotes the $N \times N$ identity matrix, $\mathrm{diag}(\mathbf{A}_1, \cdots, \mathbf{A}_L)$ is a block diagonal matrix with $\mathbf{A}_1, \cdots, \mathbf{A}_L$ on the diagonal, and $\mathrm{toeplitz}(\mathbf{A}_{N\times M}, L)$ refers to a $NL \times (M + L - 1)$ block-Toeplitz matrix defined by $\mathrm{toeplitz}(\mathbf{A}_{N\times M}, L) \triangleq [\mathbf{A}_0^T \cdots \mathbf{A}_{L-1}^T]^T$ where $\mathbf{A}_l \triangleq [\mathbf{0}_{N\times l}\ \mathbf{A}_{N\times M}\ \mathbf{0}_{N\times(L-1-l)}]$.

2. System Model

Figure 1 shows the FD-FF relaying network consisting of a source node $\mathcal{S}$, destination node $\mathcal{D}$, and R relay nodes $\mathcal{R}_r, r = 1, \cdots, R$. Both $\mathcal{S}$ and $\mathcal{D}$ have a single antenna, and each $\mathcal{R}_r$ has N_r receiving antennas and one transmission antenna. $\mathcal{R}_r$ also has a MISO-FIR filter of length L_w. We assume that all channels, which are modeled by FIR filters, are frequency-selective and cause severe ISI, and that no direct link exists between $\mathcal{S}$ and $\mathcal{D}$ because of pathloss and shadowing. We also assume that a central node, which is placed near relay nodes, has the full/partial channel state information (CSI) of all channels. The central node determines the filter coefficients based on the CSI and then feeds them back to the relay nodes. The number of required relay nodes should be determined by the required system performance and total cost.

$\mathcal{S}$ broadcasts a source signal s_k to $\mathcal{R}_r$s at discrete time k. The source signal s_k is an i.i.d. random process taken from a PSK or QAM constellation. The transmitted signal is passed through frequency-selective channels and is received by the relay nodes. Each relay node also receives SI from its transmitter and IRI from the other nodes' transmitters. The received signals at the rth relay node $\mathcal{R}_r$ at time k is expressed as

$$\mathbf{r}_{r,k} = \sum_{l=0}^{L_\mathrm{f}-1} \mathbf{f}_{r,l} s_{k-l} + \sum_{i=1}^{R} \sum_{l=0}^{L_{r,i}-1} \mathbf{h}_{r,i,l} t_{i,k-l} + \mathbf{n}_{r,k}. \quad (1)$$

The first term represents the signal from $\mathcal{S}$, which contains a desired symbol and ISI. The second term represents the signals from $\mathcal{R}_i$s, which contain SI from $\mathcal{R}_r$ and IRI from $\mathcal{R}_i, i \neq r$ (we refer to the sum of SI and IRI as loop interference (LI)). Finally, the third term represents noise. In (1), $\mathbf{r}_{r,k} \triangleq [r_{r,k}^{(1)} \cdots r_{r,k}^{(N_\mathrm{r})}]^T$, $r_{r,k}^{(n)}$ is the received signal of the nth receive antenna, $\mathbf{f}_{r,l} \triangleq [f_{r,l}^{(1)} \cdots f_{r,l}^{(N_\mathrm{r})}]^T$, $f_{r,l}^{(n)}$ is the lth path gain of the channel impulse response (CIR) between $\mathcal{S}$ and the nth receive antenna of $\mathcal{R}_r$, L_f is the CIR length of the $\mathcal{S}$-$\mathcal{R}_r$ channels, $\mathbf{h}_{r,i,l} \triangleq [h_{r,i,l}^{(1)} \cdots h_{r,i,l}^{(N_\mathrm{r})}]^T$, $h_{r,i,l}^{(n)}$ is the lth path gain of the CIR between the transmit antenna of $\mathcal{R}_i$ and the nth receive antenna of $\mathcal{R}_r$, $L_{r,i}$ is the CIR length of $\mathcal{R}_i$-$\mathcal{R}_r$ channels, $t_{i,k}$ is the transmitted signal from $\mathcal{R}_i$, and $\mathbf{n}_{r,k} \triangleq [n_{r,k}^{(1)} \cdots n_{r,k}^{(N_\mathrm{r})}]^T$ is the noise at $\mathcal{R}_r$. Note that the loop-back channel $\mathbf{h}_{r,r,l}$ causes SI, and the inter-relay channel $\mathbf{h}_{r,i,l}$ for $r \neq i$ causes IRI.

In $\mathcal{R}_r$, the received signal $\mathbf{r}_{r,k}$ is processed by the MISO-FIR filter to suppress LI and ISI jointly. Then, $\mathcal{R}_r$ forwards the filtered signal to $\mathcal{D}$. The transmitted signal from $\mathcal{R}_r$ is represented by

$$t_{r,k} \triangleq \sum_{l=0}^{L_\mathrm{w}-1} \mathbf{w}_{r,l}^H \mathbf{r}_{r,k-l-d} \quad (2)$$

where $\mathbf{w}_{r,l} \triangleq [w_{r,l}^{(1)} \cdots w_{r,l}^{(N_\mathrm{r})}]^T$ is the lth tap coefficients of the MISO-FIR filter at $\mathcal{R}_r$, and L_w is the length of the relay filter. In (2), the received signal is delayed intentionally by d samples (its purpose is explained later in Sect. 3). We can rewrite (2) as (the derivation is shown in the Appendix)

$$t_{r,k} = \mathbf{w}_r^H (\bar{\mathbf{F}}_r \bar{\mathbf{s}}_{k-d} + \bar{\mathbf{H}}_r \bar{\mathbf{t}}_{k-d} + \bar{\mathbf{n}}_{r,k-d}) \quad (3)$$

where

$$\begin{aligned}
&\mathbf{w}_r \triangleq [\mathbf{w}_{r,0}^T \cdots \mathbf{w}_{r,L_\mathrm{w}-1}^T]^T,\\
&\bar{\mathbf{s}}_k \triangleq [s_k \cdots s_{k-L_\mathrm{f}-L_\mathrm{w}+2}]^T, \bar{\mathbf{t}}_k \triangleq [\bar{\mathbf{t}}_{1,k}^T \cdots \bar{\mathbf{t}}_{R,k}^T]^T,\\
&\bar{\mathbf{t}}_{r,k} \triangleq [t_{r,k} \cdots t_{r,k-L_\mathrm{h}-L_\mathrm{w}+2}]^T,\\
&\bar{\mathbf{n}}_{r,k} \triangleq [\mathbf{n}_{r,k}^T \cdots \mathbf{n}_{r,k-L_\mathrm{w}+1}^T]^T,\\
&\bar{\mathbf{F}}_r \triangleq \mathrm{toeplitz}(\mathbf{F}_r, L_\mathrm{w}), \mathbf{F}_r \triangleq [\mathbf{f}_{r,0} \cdots \mathbf{f}_{r,L_\mathrm{f}-1}],\\
&\bar{\mathbf{H}}_r \triangleq [\bar{\mathbf{H}}_{r,1} \cdots \bar{\mathbf{H}}_{r,R}], \bar{\mathbf{H}}_{r,i} \triangleq \mathrm{toeplitz}(\mathbf{H}_{r,i}, L_\mathrm{w}),\\
&\mathbf{H}_{r,i} \triangleq [\mathbf{h}_{r,i,0} \cdots \mathbf{h}_{r,i,L_{r,i}-1}\ \mathbf{0}_{N_\mathrm{r}\times(L_\mathrm{h}-L_{r,i})}],\\
&L_\mathrm{h} \triangleq \max_{r,i} L_{r,i}.
\end{aligned}$$

The received signal at $\mathcal{D}$ is given by

$$y_k \triangleq \sum_{r=1}^{R} \sum_{l=0}^{L_\mathrm{g}-1} g_{r,l} t_{r,k-l} + v_k \quad (4)$$

where $g_{r,l}$ is the lth path gain of the CIR between $\mathcal{R}_r$ and $\mathcal{D}$, L_g is the CIR length of the $\mathcal{R}_r$-$\mathcal{D}$ channels, and v_k is the noise at $\mathcal{D}$. We can rewrite (4) as (the derivation is shown in the Appendix)

$$y_k = \sum_{r=1}^{R} \mathbf{g}_r^T \breve{\mathbf{W}}_r^H (\breve{\mathbf{F}}_r \breve{\mathbf{s}}_{k-d} + \breve{\mathbf{H}}_r \breve{\mathbf{t}}_{k-d} + \bar{\mathbf{I}} \breve{\mathbf{n}}_{r,k-d}) + v_k \quad (5)$$

$$= \mathbf{g}^T \breve{\mathbf{W}}^H (\breve{\mathbf{F}} \breve{\mathbf{s}}_{k-d} + \breve{\mathbf{H}} \breve{\mathbf{t}}_{k-d} + \breve{\mathbf{I}} \breve{\mathbf{n}}_{k-d}) + v_k \quad (6)$$

$$= \mathbf{w}^H \breve{\mathbf{G}} (\breve{\mathbf{F}} \breve{\mathbf{s}}_{k-d} + \breve{\mathbf{H}} \breve{\mathbf{t}}_{k-d} + \breve{\mathbf{I}} \breve{\mathbf{n}}_{k-d}) + v_k \quad (7)$$

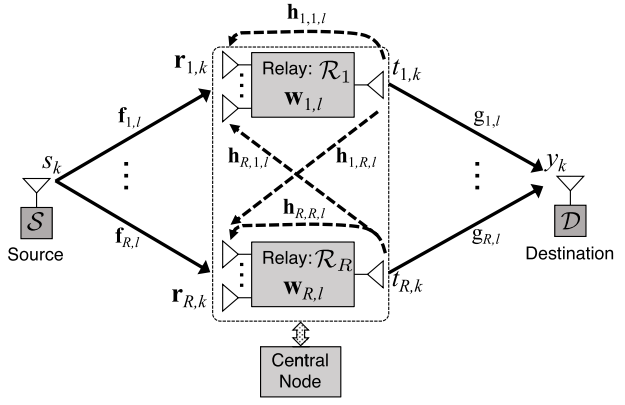

Fig. 1 Filter-and-forward-based full-duplex (FF-FD) relaying network.

where

$$\check{\mathbf{W}}_r \triangleq \mathbf{I}_{L_\mathrm{g}} \otimes \mathbf{w}_r, \check{\mathbf{W}} \triangleq \mathrm{diag}(\check{\mathbf{W}}_1, \cdots, \check{\mathbf{W}}_R),$$
$$\mathbf{w} \triangleq [\mathbf{w}_1^T \ \cdots \mathbf{w}_R^T]^T,$$
$$\check{\mathbf{s}}_k \triangleq [s_k \ \cdots s_{k-L_\mathrm{f}-L_\mathrm{w}-L_\mathrm{g}+3}]^T,$$
$$\check{\mathbf{t}}_k \triangleq [\check{\mathbf{t}}_{1,k}^T \ \cdots \ \check{\mathbf{t}}_{R,k}^T]^T, \check{\mathbf{n}}_k \triangleq [\check{\mathbf{n}}_{1,k}^T \ \cdots \ \check{\mathbf{n}}_{R,k}^T]^T,$$
$$\check{\mathbf{t}}_{r,k} \triangleq [t_{r,k} \ \cdots \ t_{r,k-L_\mathrm{h}-L_\mathrm{w}-L_\mathrm{g}+3}]^T,$$
$$\check{\mathbf{n}}_{r,k} \triangleq [\mathbf{n}_{r,k}^T \ \cdots \ \mathbf{n}_{r,k-L_\mathrm{w}-L_\mathrm{g}+2}^T]^T,$$
$$\check{\mathbf{G}} \triangleq \mathrm{diag}(\check{\mathbf{G}}_1, \cdots, \check{\mathbf{G}}_R), \check{\mathbf{G}}_r \triangleq \mathbf{g}_r^T \otimes \mathbf{I}_{N_\mathrm{r}L_\mathrm{w}},$$
$$\mathbf{g}_r \triangleq [g_{r,0} \ \cdots \ g_{r,L_\mathrm{g}-1}]^T, \mathbf{g} \triangleq [\mathbf{g}_1^T \ \cdots \ \mathbf{g}_R^T]^T,$$
$$\check{\mathbf{F}} \triangleq [\check{\mathbf{F}}_1^T \ \cdots \ \check{\mathbf{F}}_R^T]^T, \check{\mathbf{F}}_r \triangleq \mathrm{toeplitz}(\bar{\mathbf{F}}_r, L_\mathrm{g}),$$
$$\check{\mathbf{H}} \triangleq [\check{\mathbf{H}}_1^T \ \cdots \ \check{\mathbf{H}}_R^T]^T, \check{\mathbf{H}}_r \triangleq [\check{\mathbf{H}}_{r,1} \ \cdots \ \check{\mathbf{H}}_{r,R}],$$
$$\check{\mathbf{H}}_{r,i} \triangleq \mathrm{toeplitz}(\bar{\mathbf{H}}_{r,i}, L_\mathrm{g}),$$
$$\check{\mathbf{I}} \triangleq \mathbf{I}_R \otimes \bar{\mathbf{I}}, \bar{\mathbf{I}} \triangleq [\bar{\mathbf{I}}_0^T \ \cdots \ \bar{\mathbf{I}}_{L_\mathrm{g}-1}^T]^T,$$
$$\bar{\mathbf{I}}_l \triangleq [\mathbf{0}_{N_\mathrm{r}L_\mathrm{w} \times N_\mathrm{r}l} \ \mathbf{I}_{N_\mathrm{r}L_\mathrm{w}} \ \mathbf{0}_{N_\mathrm{r}L_\mathrm{w} \times N_\mathrm{r}(L_\mathrm{g}-1-l)}].$$

The first term of (7) $\mathbf{w}^H\check{\mathbf{G}}\check{\mathbf{F}}\check{\mathbf{s}}_{k-d}$ contains the desired symbol and ISI. We regard an element of $\check{\mathbf{s}}_{k-d}$, say s_{k-d-p}, as the desired symbol. Then, the decision at $\mathcal{D}$ is delayed by $p+d$ samples (i.e., the decision based on y_k produces the estimation of s_{k-d-p}). The remaining symbols in $\check{\mathbf{s}}_{k-d}$ are regarded as ISI. We can rewrite (7) as

$$y_k = \underbrace{\mathbf{w}^H\check{\mathbf{G}}\tilde{\mathbf{f}}s_{k-d-p}}_{y_{\mathrm{D},k}:\text{desired symbol}} + \underbrace{\mathbf{w}^H\check{\mathbf{G}}\tilde{\mathbf{F}}\check{\mathbf{s}}_{k-d}}_{y_{\mathrm{ISI},k}:\text{ISI}} + \underbrace{\mathbf{w}^H\check{\mathbf{G}}\check{\mathbf{H}}\check{\mathbf{t}}_{k-d}}_{y_{\mathrm{LI},k}:\text{SI + IRI}} + \underbrace{\mathbf{w}^H\check{\mathbf{G}}\check{\mathbf{I}}\check{\mathbf{n}}_{k-d} + v_k}_{y_{\mathrm{N},k}:\text{noises}} \quad (8)$$

where $\tilde{\mathbf{f}}$ is the $(p+1)$th column of $\check{\mathbf{F}}$, $\tilde{\mathbf{F}} \triangleq [\tilde{\mathbf{F}}_1 \ \tilde{\mathbf{F}}_2]$, $\check{\mathbf{F}} = [\tilde{\mathbf{F}}_1 \ \tilde{\mathbf{f}} \ \tilde{\mathbf{F}}_2]$, $\tilde{\mathbf{s}}_{k-d} \triangleq [\tilde{\mathbf{s}}_{k-d,1}^T \ \tilde{\mathbf{s}}_{k-d,2}^T]^T$, and $\check{\mathbf{s}}_{k-d} = [\tilde{\mathbf{s}}_{k-d,1}^T \ s_{k-d-p} \ \tilde{\mathbf{s}}_{k-d,2}^T]^T$. In (8), there are four terms: the desired symbol $y_{\mathrm{D},k}$, ISI $y_{\mathrm{ISI},k}$, LI $y_{\mathrm{LI},k}$, and noise $y_{\mathrm{N},k}$ components. The purpose of filter design is to determine the relay filter coefficient vector $\mathbf{w}$ such that the interference components (ISI+LI) are suppressed while the desired symbol is enhanced.

3. Filter Design with Full CSI

We consider determining the filter coefficients $\mathbf{w}$ in a case in which full CSI (i.e., instantaneous CIR of all channels) is available. Our approach is based on the maximization of SINR at $\mathcal{D}$ subject to the constraint that the total relay transmission power remains below a predetermined limit. We assume that external power sources supply sufficient power to all the relay nodes to meet the total relay transmission power constraint[†]. The problem can be formulated as follows

$$\max_{\mathbf{w}} \ \mathrm{SINR} \ \text{ s.t. } P_\mathrm{R} \le P_\mathrm{max} \quad (9)$$

where P_max is the predetermined maximum value of the total relay transmission power $P_\mathrm{R} \triangleq \sum_{r=1}^{R} \mathrm{E}[|t_{r,k}|^2]$. As shown in (2), we intentionally delay the received signal at the relays by d, which is chosen such that

$$d > L_\mathrm{f} + L_\mathrm{w} + L_\mathrm{g} - 2. \quad (10)$$

Under this condition, the ISI component $y_{\mathrm{ISI},k}$ and LI component $y_{\mathrm{LI},k}$ in (8) do not share any common symbols s_k, and thus $y_{\mathrm{ISI},k}$ is uncorrelated with $y_{\mathrm{LI},k}$ (i.e., $\mathrm{E}[y_{\mathrm{ISI},k}\, y_{\mathrm{LI},k}^*] = 0$). Then, at the expense of processing delay, we can simplify the expression of a receive SINR at $\mathcal{D}$ as

$$\mathrm{SINR} \triangleq \frac{P_\mathrm{D}}{P_\mathrm{ISI} + P_\mathrm{LI} + P_\mathrm{N}} \quad (11)$$

where $P_\mathrm{D} = \mathrm{E}[|y_{\mathrm{D},k}|^2]$, $P_\mathrm{ISI} = \mathrm{E}[|y_{\mathrm{ISI},k}|^2]$, $P_\mathrm{LI} = \mathrm{E}[|y_{\mathrm{LI},k}|^2]$, and $P_\mathrm{N} = \mathrm{E}[|y_{\mathrm{N},k}|^2]$. When the full CSI is available, from (3) and (8), SINR and P_R can be written as

$$\mathrm{SINR} = \frac{\mathbf{w}^H\mathbf{Q}_\mathrm{D}\mathbf{w}}{\mathbf{w}^H(\mathbf{Q}_\mathrm{ISI} + \mathbf{Q}_\mathrm{LI} + \mathbf{Q}_\mathrm{N})\mathbf{w} + \sigma^2} \quad (12)$$

$$P_\mathrm{R} = \sum_{r=1}^{R} \mathbf{w}^H\mathbf{E}_r(P_\mathrm{s}\bar{\mathbf{F}}\bar{\mathbf{F}}^H + \bar{\mathbf{H}}\bar{\mathbf{R}}_\mathrm{t}\bar{\mathbf{H}}^H + \sigma^2\mathbf{I}_{RN_\mathrm{r}L_\mathrm{w}})\mathbf{E}_r^H\mathbf{w} \quad (13)$$

where $\mathbf{Q}_\mathrm{D} \triangleq P_\mathrm{s}\check{\mathbf{G}}\tilde{\mathbf{f}}\tilde{\mathbf{f}}^H\check{\mathbf{G}}^H$, $\mathbf{Q}_\mathrm{ISI} \triangleq P_\mathrm{s}\check{\mathbf{G}}\tilde{\mathbf{F}}\tilde{\mathbf{F}}^H\check{\mathbf{G}}^H$, $\mathbf{Q}_\mathrm{LI} \triangleq \check{\mathbf{G}}\check{\mathbf{H}}\check{\mathbf{R}}_\mathrm{t}\check{\mathbf{H}}^H\check{\mathbf{G}}^H$, $\mathbf{Q}_\mathrm{N} \triangleq \sigma^2\check{\mathbf{G}}\check{\mathbf{I}}\check{\mathbf{I}}^H\check{\mathbf{G}}^H$, $P_\mathrm{s} \triangleq \mathrm{E}[|s_k|^2]$ is the transmitted power of the source, $\check{\mathbf{R}}_\mathrm{t} \triangleq \mathrm{E}[\check{\mathbf{t}}_{k-d}\check{\mathbf{t}}_{k-d}^H]$ and $\bar{\mathbf{R}}_\mathrm{t} \triangleq \mathrm{E}[\bar{\mathbf{t}}_{k-d}\bar{\mathbf{t}}_{k-d}^H]$ are the correlation matrices of the relay transmitted signals, $\mathbf{E}_r = \mathbf{I}_{N_\mathrm{r}L_\mathrm{w}} \otimes \mathbf{E}'_r$, $\mathbf{E}'_r$ is the $R \times R$ matrix whose elements are zeros except the (r,r) element, which is one, $\bar{\mathbf{F}} \triangleq [\bar{\mathbf{F}}_1^T \ \cdots \ \bar{\mathbf{F}}_R^T]^T$, and $\bar{\mathbf{H}} \triangleq [\bar{\mathbf{H}}_1^T \ \cdots \ \bar{\mathbf{H}}_R^T]^T$. The noises are assumed to be white Gaussian with the power $\sigma^2 \triangleq \mathrm{E}[|n_{r,k}^{(n)}|^2] = \mathrm{E}[|v_k|^2]$ for $r = 1, \cdots, R, n = 1, \cdots, N_\mathrm{r}$.

To obtain $\mathbf{w}$ by solving the problem (9) using (12) and (13), we must evaluate the contributions of LI (i.e., $\mathbf{w}^H\mathbf{Q}_\mathrm{LI}\mathbf{w}$ and $\mathbf{w}^H\sum_{r=1}^{R}(\mathbf{E}_r\bar{\mathbf{H}}\bar{\mathbf{R}}_\mathrm{t}\bar{\mathbf{H}}^H\mathbf{E}_r^H)\mathbf{w}$). They include the correlation matrices $\check{\mathbf{R}}_\mathrm{t}$ and $\bar{\mathbf{R}}_\mathrm{t}$, which are difficult to obtain because they are affected by the filter coefficients $\mathbf{w}$. To avoid this issue, we propose two approaches. In the first approach, we impose a constraint on the filter coefficients so that the filter responses to LI are forced to zero. In the second approach, we make a statistical assumption based on the relay transmitted signals $t_{r,k}$ to simplify the correlation matrices.

3.1 Method A: LI Nulling Approach

We add a constraint to the problem (9), which ensures com-

[†]The total relay transmission power constraint has been widely considered in the literature on relay networks [11], [12], [14], [15]. To realize the total transmission power constraint, we assume that a central node and external power sources for relay nodes are used at the expense of increased system cost. In the case where small relay nodes such as simple sensor nodes or mobile hand-held devices are restricted in their battery lifetimes, individual relay power constraints are preferable. Such approaches can be found for half-duplex transmission [11], [14].

plete suppression of LI at the FIR filter output. Specifically, from (3), we impose the interference nulling constraint $\mathbf{w}_r^H \bar{\mathbf{H}}_r \bar{\mathbf{t}}_{k-d} = 0$ for all r and k. We rewrite the constraint using the filter coefficients $\mathbf{w}$ as

$$\mathbf{w}^H \tilde{\mathbf{H}} (\mathbf{I}_R \otimes \bar{\mathbf{t}}_{k-d}) = \mathbf{0} \tag{14}$$

for all k, where $\tilde{\mathbf{H}} \triangleq \mathrm{diag}(\bar{\mathbf{H}}_1, \cdots, \bar{\mathbf{H}}_R)$. We have a sufficient condition for satisfying (14):

$$\tilde{\mathbf{H}}^H \mathbf{w} = \mathbf{0}. \tag{15}$$

We employ (15) as the constraint.

Because of the nulling constraint, the contributions of LI to SINR in (12) and P_R in (13) vanish (i.e., we have $\mathbf{w}^H \mathbf{Q}_{\mathrm{LI}} \mathbf{w} = 0$ and $\mathbf{w}^H \sum_{r=1}^{R} (\mathbf{E}_r \bar{\mathbf{H}} \bar{\mathbf{R}}_{\mathrm{t}} \bar{\mathbf{H}}^H \mathbf{E}_r^H) \mathbf{w} = 0$). We then have the modified problem given by

$$\begin{aligned} &\max_{\mathbf{w}} \ \mathrm{SINR} = \frac{\mathbf{w}^H \mathbf{Q}_{\mathrm{D}} \mathbf{w}}{\mathbf{w}^H (\mathbf{Q}_{\mathrm{ISI}} + \mathbf{Q}_{\mathrm{N}}) \mathbf{w} + \sigma^2} \\ &\text{s.t. } P_{\mathrm{R}} = \mathbf{w}^H \mathbf{D}_{\mathrm{A}} \mathbf{w} \le P_{\max}, \ \tilde{\mathbf{H}}^H \mathbf{w} = \mathbf{0} \end{aligned} \tag{16}$$

where $\mathbf{D}_{\mathrm{A}} \triangleq \sum_{r=1}^{R} \mathbf{E}_r (P_{\mathrm{s}} \bar{\mathbf{F}} \bar{\mathbf{F}}^H + \sigma^2 \mathbf{I}_{RN_{\mathrm{r}}L_{\mathrm{w}}}) \mathbf{E}_r^H$. Denoting $\tilde{\mathbf{w}}_{\mathrm{A}} = \mathbf{D}_{\mathrm{A}}^{1/2} \mathbf{w}$, we can further rewrite (16) as

$$\begin{aligned} &\max_{\tilde{\mathbf{w}}_{\mathrm{A}}} \ \frac{\tilde{\mathbf{w}}_{\mathrm{A}}^H \tilde{\mathbf{Q}}_{\mathrm{D,A}} \tilde{\mathbf{w}}_{\mathrm{A}}}{\tilde{\mathbf{w}}_{\mathrm{A}}^H \tilde{\mathbf{Q}}_{\mathrm{IN,A}} \tilde{\mathbf{w}}_{\mathrm{A}} + \sigma^2} \\ &\text{s.t. } \|\tilde{\mathbf{w}}_{\mathrm{A}}\|^2 \le P_{\max}, \ \tilde{\mathbf{H}}^H \mathbf{D}_{\mathrm{A}}^{-1/2} \tilde{\mathbf{w}}_{\mathrm{A}} = \mathbf{0} \end{aligned} \tag{17}$$

where $\tilde{\mathbf{Q}}_{\mathrm{D,A}} \triangleq \mathbf{D}_{\mathrm{A}}^{-1/2} \mathbf{Q}_{\mathrm{D}} \mathbf{D}_{\mathrm{A}}^{-1/2}$ and $\tilde{\mathbf{Q}}_{\mathrm{IN,A}} \triangleq \mathbf{D}_{\mathrm{A}}^{-1/2} (\mathbf{Q}_{\mathrm{ISI}} + \mathbf{Q}_{\mathrm{N}}) \mathbf{D}_{\mathrm{A}}^{-1/2}$.

The second constraint in (17) implies that $\tilde{\mathbf{w}}_{\mathrm{A}}$ belongs to a space orthogonal to the LI component $\tilde{\mathbf{H}}^H \mathbf{D}_{\mathrm{A}}^{-1/2}$. This constraint can be dropped by introducing a projection matrix $\mathbf{K}$ that satisfies $\tilde{\mathbf{H}}^H \mathbf{D}_{A}^{-1/2} \mathbf{K} = \mathbf{0}$. When we project an alternative filter coefficient vector $\hat{\mathbf{w}}_{\mathrm{A}}$ onto a space orthogonal to the LI component as $\mathbf{K}\hat{\mathbf{w}}_{\mathrm{A}} = \tilde{\mathbf{w}}_{\mathrm{A}}$, $\tilde{\mathbf{H}}^H \mathbf{D}_{\mathrm{A}}^{-1/2} \mathbf{K} \hat{\mathbf{w}}_{\mathrm{A}} = \mathbf{0}$ holds for any $\hat{\mathbf{w}}_{\mathrm{A}}$. We choose $\mathbf{K}$ such that $\mathbf{K}^H \mathbf{K} = \mathbf{I}$. Note that the objective function in (17) monotonically increases as $P_{\mathrm{R}} (= \|\tilde{\mathbf{w}}_{\mathrm{A}}\|^2)$ increases[†]. Thus, the objective function achieves its maximum when P_{R} is its maximum $P_{\max}$. Therefore, we can replace the constraint $\|\tilde{\mathbf{w}}_{\mathrm{A}}\|^2 \le P_{\max}$ in (17) by $\|\hat{\mathbf{w}}_{\mathrm{A}}\|^2 = P_{\max}$. We can now reformulate (17) as

$$\max_{\hat{\mathbf{w}}_{\mathrm{A}}} \ \frac{\hat{\mathbf{w}}_{\mathrm{A}}^H \mathbf{K}^H \tilde{\mathbf{Q}}_{\mathrm{D,A}} \mathbf{K} \hat{\mathbf{w}}_{\mathrm{A}}}{\hat{\mathbf{w}}_{\mathrm{A}}^H \mathbf{K}^H \tilde{\mathbf{Q}}_{\mathrm{INN,A}} \mathbf{K} \hat{\mathbf{w}}_{\mathrm{A}}} \ \text{s.t. } \|\hat{\mathbf{w}}_{\mathrm{A}}\|^2 = P_{\max} \tag{18}$$

where $\tilde{\mathbf{Q}}_{\mathrm{INN,A}} \triangleq \tilde{\mathbf{Q}}_{\mathrm{IN,A}} + (\sigma^2 / P_{\max}) \mathbf{I}$. The resulting problem (18) can be solved as a generalized eigenvalue problem [11]. Finally, we obtain the optimal filter coefficients as

$$\mathbf{w}_{\mathrm{opt,A}} = \sqrt{P_{\max}} \mathbf{D}_{\mathrm{A}}^{-1/2} \mathbf{K} \times \mathcal{P}_{\max} \{ \mathbf{K}^H \tilde{\mathbf{Q}}_{\mathrm{D,A}} \mathbf{K}, \mathbf{K}^H \tilde{\mathbf{Q}}_{\mathrm{INN,A}} \mathbf{K} \} \tag{19}$$

where $\mathcal{P}_{\max}\{\mathbf{A}, \mathbf{B}\}$ denotes the normalized generalized eigenvector corresponding to the largest generalized eigenvalue of the matrix pair $(\mathbf{A}, \mathbf{B})$.

Note that the projection matrix $\mathbf{K}$, whose size is $RN_{\mathrm{r}}L_{\mathrm{w}} \times (RN_{\mathrm{r}}L_{\mathrm{w}} - \rho)$, where $\rho = \mathrm{rank}(\tilde{\mathbf{H}}^H \mathbf{D}_{\mathrm{A}}^{-1/2}) = \mathrm{rank}(\tilde{\mathbf{H}})$, can be obtained by singular-value decomposition of $\tilde{\mathbf{H}}^H \mathbf{D}_{\mathrm{A}}^{-1/2}$. The complete suppression of LI is ensured only when $\mathbf{K}$ exists. A sufficient condition for the existence of $\mathbf{K}$ is that $\tilde{\mathbf{H}}$ (whose size is $RN_{\mathrm{r}}L_{\mathrm{w}} \times (L_{\mathrm{h}} + L_{\mathrm{w}} - 1)R^2$) must be tall, that is

$$N_{\mathrm{r}}L_{\mathrm{w}} > (L_{\mathrm{h}} + L_{\mathrm{w}} - 1)R. \tag{20}$$

This condition can be satisfied by increasing the number of receive antennas N_{r} at each relay. In addition, sufficient ISI suppression requires a greater number of antennas or longer filters, which increase system complexity. Also, this method is susceptible to noise enhancement, particularly when the length of filters is short, as described in Sect. 5.

The computational complexity in terms of required number of multiplications is largely dominated by the computation of $\mathbf{D}_{\mathrm{A}}^{-1/2}$, $\tilde{\mathbf{Q}}_{\mathrm{D,A}}$, and $\tilde{\mathbf{Q}}_{\mathrm{IN,A}}$. Their complexity is proportional to $(RN_{\mathrm{r}}L_{\mathrm{w}})^3$. Additionally, this method requires the generalized eigenvalue decomposition (GEVD) in (19), whose complexity is $O((RN_{\mathrm{r}}L_{\mathrm{w}} - \rho)^3)$.

3.2 Method B: I.I.D. Approximation Approach

The correlation matrices $\breve{\mathbf{R}}_{\mathrm{t}}$ and $\bar{\mathbf{R}}_{\mathrm{t}}$ depend on the statistics of the relay transmitted signals $t_{r,k}$, but unfortunately, we cannot obtain the correct statistics. Here, we take a crude approach that makes the i.i.d. approximation on $t_{r,k}$. This approximation results in the following: 1) the transmitted signals of different relays are uncorrelated with each other, 2) the transmitted signal of each relay is an uncorrelated sequence, 3) the transmission power of each relay is identical. Because of these results, we can simplify the correlation matrices as

$$\breve{\mathbf{R}}_{\mathrm{t}} = \frac{P_{\mathrm{R}}}{R} \mathbf{I}_{L_{\mathrm{h}}+L_{\mathrm{w}}+L_{\mathrm{g}}-2}, \ \bar{\mathbf{R}}_{\mathrm{t}} = \frac{P_{\mathrm{R}}}{R} \mathbf{I}_{L_{\mathrm{h}}+L_{\mathrm{w}}-1}. \tag{21}$$

Using (12), (13), and (21), we can obtain

$$P_{\mathrm{LI}} = \mathbf{w}^H \underbrace{((P_{\mathrm{R}}/R) \breve{\mathbf{G}} \bar{\mathbf{H}} \breve{\mathbf{H}}^H \breve{\mathbf{G}}^H)}_{\mathbf{Q}_{\mathrm{LI}}} \mathbf{w} \tag{22}$$

$$P_R = \mathbf{w}^H \mathbf{D}_{\mathrm{B}} \mathbf{w} \tag{23}$$

where $\mathbf{D}_{\mathrm{B}} \triangleq \sum_{r=1}^{R} \mathbf{E}_r (P_{\mathrm{s}} \bar{\mathbf{F}} \bar{\mathbf{F}}^H + (P_{\mathrm{R}}/R) \bar{\mathbf{H}} \bar{\mathbf{H}}^H + \sigma^2 \mathbf{I}_{RN_{\mathrm{r}}L_{\mathrm{w}}}) \mathbf{E}_r^H$. However, determining $\mathbf{Q}_{\mathrm{LI}}$ and $\mathbf{D}_{\mathrm{B}}$ remains cumbersome because they require P_{R}, which is a quadratic function of $\mathbf{w}$. One might think that P_R can be set to its maximum $P_{\max}$. However, this is not a good choice because the actual transmit power P_R often exceeds $P_{\max}$ due to the rough i.i.d. approximation. To avoid this difficulty, we propose an optimization procedure in which the filter coefficients $\mathbf{w}$ and the

[†]This is justified by the fact that it can be written as $\frac{P_{\mathrm{R}} \bar{\mathbf{w}}_{\mathrm{A}}^H \tilde{\mathbf{Q}}_{\mathrm{D,A}} \bar{\mathbf{w}}_{\mathrm{A}}}{P_{\mathrm{R}} \bar{\mathbf{w}}_{\mathrm{A}}^H \tilde{\mathbf{Q}}_{\mathrm{IN,A}} \bar{\mathbf{w}}_{\mathrm{A}} + \sigma^2}$ where $\bar{\mathbf{w}}_{\mathrm{A}} = \tilde{\mathbf{w}}_{\mathrm{A}} / \sqrt{P_{\mathrm{R}}}$ and $\|\bar{\mathbf{w}}_{\mathrm{A}}\|^2 = 1$.

relay transmit power P_{R} are alternately determined.

First, let us explain how to optimize $\mathbf{w}$ when the transmit power is given as $P_{\mathrm{R}} = P'$, where P' is called "temporary power" and $P' \leq P_{\max}$. Using (22) and (23), and introducing $\tilde{\mathbf{w}}_{\mathrm{B}} = \mathbf{D}_{\mathrm{B},P'}^{1/2}\mathbf{w}$, $\mathbf{D}_{\mathrm{B},P'} \triangleq \mathbf{D}_{\mathrm{B}}|_{P_{\mathrm{R}}=P'}$, we can rewrite (9) as

$$\max_{\tilde{\mathbf{w}}_{\mathrm{B}}} \frac{\tilde{\mathbf{w}}_{\mathrm{B}}^H \tilde{\mathbf{Q}}_{\mathrm{D,B}} \tilde{\mathbf{w}}_{\mathrm{B}}}{\tilde{\mathbf{w}}_{\mathrm{B}}^H \tilde{\mathbf{Q}}_{\mathrm{IN,B}} \tilde{\mathbf{w}}_{\mathrm{B}}} \quad \text{s.t. } \|\tilde{\mathbf{w}}_{\mathrm{B}}\|^2 = P' \leq P_{\max} \tag{24}$$

where $\tilde{\mathbf{Q}}_{\mathrm{D,B}} \triangleq \mathbf{D}_{\mathrm{B},P'}^{-1/2}\mathbf{Q}_{\mathrm{D}}\mathbf{D}_{\mathrm{B},P'}^{-1/2}$, $\tilde{\mathbf{Q}}_{\mathrm{IN,B}} \triangleq \mathbf{D}_{\mathrm{B},P'}^{-1/2}(\mathbf{Q}_{\mathrm{ISI}} + \mathbf{Q}_{\mathrm{LI},P'} + \mathbf{Q}_{\mathrm{N}})\mathbf{D}_{\mathrm{B},P'}^{-1/2} + (\sigma^2/P')\mathbf{I}_{RN_{\mathrm{r}}L_{\mathrm{w}}}$, $\mathbf{Q}_{\mathrm{LI},P'} \triangleq \mathbf{Q}_{\mathrm{LI}}|_{P_{\mathrm{R}}=P'}$. This problem can be solved in a similar manner to that for (18), where the solution is given as

$$\mathbf{w}_{\mathrm{B}}(P') = \sqrt{P'}\mathbf{D}_{\mathrm{B},P'}^{-1/2}\mathcal{P}_{\max}\{\tilde{\mathbf{Q}}_{\mathrm{D,B}}, \tilde{\mathbf{Q}}_{\mathrm{IN,B}}\}. \tag{25}$$

Equation (25) represents an optimal filter coefficient vector when the relay transmit power is $P_{\mathrm{R}} = P'$.

We next consider the optimization of the relay transmit power. We propose an iterative power optimization (IPO) algorithm, as shown in Table 1. The algorithm has two phases:

1. In the first phase, given the power limit $P_{\max}$, we find the maximum temporary power $P'_{\max}$, which does not exceed $P_{\max}$. We measure the actual transmit power $\check{P}$ using N transmit samples of the relays that own the filter derived from (25). Using the measurements $\check{P}$, we find the maximum power $P'_{\max}$ by the bisection search with a tolerance parameter ϵ_1, which is a small positive number.
2. Unlike the nulling approach described in Sect. 3.1, SINR does not monotonically increase as the relay transmit power increases. Thus, $P'_{\max}$ obtained in the first phase is not always optimal. Through preliminary simulations, we found that SINR is a unimodal function of the relay transmit power.
In the second phase, we find the optimal power P'_{opt}, which maximizes SINR, from the range $[0, P'_{\max}]$. We calculate SINRs using (12) for the filters obtained by (25). Because SINR is a unimodal function of the relay transmit power, we can find the optimal power P'_{opt} through the golden section search [18] with a tolerance parameter ϵ_2 using the calculated SINRs.

Table 1 Iterative power optimization (IPO) algorithm.

Phase 1: Find the maximum temporary power $P'_{\max}$	
Step 1:	Initialization: $[P'_l, P'_u] = [0, P_{\max}]$, $P'_{\max} = P_{\max}/2$.
Step 2:	Calculate $\mathbf{w}_{\mathrm{B}}(P'_{\max})$ by (25).
Step 3:	Measure the actual power $\check{P} \triangleq \sum_{k=1}^{N} \|\mathbf{t}_k\|^2/N$.
Step 4:	If $\check{P} \leq P_{\max}$, $P'_l = P'_{\max}$, else $P'_u = P'_{\max}$.
Step 5:	Set $P'_{\max} = (P'_l + P'_u)/2$.
Step 6:	Repeat Steps 2–5 until $(P'_u - P'_l)/P'_l < \epsilon_1$.
Phase 2: Find the optimal power P'_{opt}	
Step 1:	Initialization: $[P'_l, P'_u] = [0, P'_{\max}]$ and $[p_l, p_u]$= $[P'_u + (P'_l - P'_u)/\phi, P'_u + (P'_l - P'_u)/(\phi + 1)]$ where $\phi = (1 + \sqrt{5})/2$.
Step 2:	Calculate $\mathbf{w}_{\mathrm{B}}(p_l)$ and $\mathbf{w}_{\mathrm{B}}(p_u)$ by (25).
Step 3:	Calculate SINR_l and SINR_u by (12) and (21) using $\mathbf{w}_{\mathrm{B}}(p_l)$ and $\mathbf{w}_{\mathrm{B}}(p_u)$, respectively.
Step 4:	If $\lvert\mathrm{SINR}_u - \mathrm{SINR}_l\rvert/\mathrm{SINR}_l \leq \epsilon_2$ go to Step 6;
Step 5:	If $\mathrm{SINR}_l < \mathrm{SINR}_u$, $P'_l = p_l$, $p_l = p_u$, $\mathrm{SINR}_l = \mathrm{SINR}_u$, $p_u = P'_u + (P'_l - P'_u)/(\phi + 1)$, Calculate $\mathbf{w}_{\mathrm{B}}(p_u)$ and SINR_u, else $P'_u = p_u$, $p_u = p_l$, $\mathrm{SINR}_u = \mathrm{SINR}_l$, $p_l = P'_u + (P'_l - P'_u)/\phi$. Calculate $\mathbf{w}_{\mathrm{B}}(p_l)$ and SINR_l. Go back to Step 4.
Step 6:	Set $P'_{\mathrm{opt}} = (p_l + p_u)/2$.

Unlike Method A, Method B is less susceptible to noise enhancement since it does not require any constraints, which limit the degree of freedom of filter design. Thus, we can expect a significant interference suppression performance compared to that of Method A.

The computational complexity per iteration of Method B, which is dominated by the computation of $\mathbf{D}_{\mathrm{B,P'}}^{-1/2}$, $\tilde{\mathbf{Q}}_{\mathrm{D,B}}$, and $\tilde{\mathbf{Q}}_{\mathrm{IN,B}}$, is proportional to $(RN_{\mathrm{r}}L_{\mathrm{w}})^3$. Additionally, the GEVD in (25), whose complexity is $O((RN_{\mathrm{r}}L_{\mathrm{w}})^3)$ is required. The computational complexity per iteration of Method B is almost the same as that of Method A. However, since Method B requires some iterations, its full complexity becomes several times higher than that of Method A.

4. Filter Design with Partial CSI

In some cases, obtaining the perfect instantaneous CSI of $\mathcal{R}_r$-$\mathcal{D}$ channels might be difficult. In this section, we apply the filter design methods proposed in Sect. 3 to a case in which only SOS of CSI regarding $\mathcal{R}_r$-$\mathcal{D}$ channels are available. We determine the filter coefficients using the instantaneous CSI of $\mathcal{S}$-$\mathcal{R}_r$ and $\mathcal{R}_r$-$\mathcal{R}_i$, and the SOS of $\mathcal{R}_r$-$\mathcal{D}$ channels without the instantaneous CSI $\check{\mathbf{G}}$.

From (6) and (11), we can rewrite the desired component power P_{D} as

$$\begin{aligned} P_{\mathrm{D}} &= P_{\mathrm{s}}\mathrm{trace}(\tilde{\mathbf{f}}^H\check{\mathbf{W}}\mathrm{E}[\mathbf{g}^*\mathbf{g}^T]\check{\mathbf{W}}^H\tilde{\mathbf{f}}) \\ &= P_{\mathrm{s}}\mathrm{trace}(\check{\mathbf{W}}^H\tilde{\mathbf{f}}\tilde{\mathbf{f}}^H\check{\mathbf{W}}\mathbf{R}_{\mathrm{g}}^*) \\ &= P_{\mathrm{s}}\mathrm{vec}(\check{\mathbf{W}}^*)^T(\mathbf{R}_{\mathrm{g}}^H \otimes \tilde{\mathbf{f}}\tilde{\mathbf{f}}^H)\mathrm{vec}(\check{\mathbf{W}}) \\ &= \mathbf{w}^H \underbrace{(P_{\mathrm{s}}\mathbf{V}^H(\mathbf{R}_{\mathrm{g}}^H \otimes \tilde{\mathbf{f}}\tilde{\mathbf{f}}^H)\mathbf{V})}_{\mathbf{Q}_{\mathrm{D}}}\mathbf{w} \end{aligned} \tag{26}$$

where $\mathbf{R}_{\mathrm{g}} \triangleq \mathrm{E}[\mathbf{g}\mathbf{g}^H]$ is the SOS of $\mathcal{R}_r$-$\mathcal{D}$ channels,

$$\begin{aligned} \mathbf{V} &\triangleq [\mathbf{V}_{1,1} \cdots \mathbf{V}_{1,L_{\mathrm{g}}} \cdots \mathbf{V}_{R,1} \cdots \mathbf{V}_{R,L_{\mathrm{g}}}]^T, \\ \mathbf{V}_{r,l} &\triangleq [\mathbf{0}_{RN_{\mathrm{r}}L_{\mathrm{w}}\times((l-1)N_{\mathrm{r}}L_{\mathrm{w}}+(r-1)N_{\mathrm{r}}L_{\mathrm{w}}L_{\mathrm{g}})}\ \tilde{\mathbf{V}}_r^T \\ &\qquad \mathbf{0}_{RN_{\mathrm{r}}L_{\mathrm{w}}\times((L_{\mathrm{g}}-l)N_{\mathrm{r}}L_{\mathrm{w}}+(R-r)N_{\mathrm{r}}L_{\mathrm{w}}L_{\mathrm{g}})}], \\ \tilde{\mathbf{V}}_r &\triangleq [\mathbf{0}_{N_{\mathrm{r}}L_{\mathrm{w}}\times(r-1)N_{\mathrm{r}}L_{\mathrm{w}}}\ \mathbf{I}_{N_{\mathrm{r}}L_{\mathrm{w}}}\ \mathbf{0}_{N_{\mathrm{r}}L_{\mathrm{w}}\times(R-r)N_{\mathrm{r}}L_{\mathrm{w}}}]. \end{aligned}$$

Similarly, P_{ISI}, P_{LI}, and P_{N} are obtained by

$$P_{\mathrm{ISI}} = \mathbf{w}^H \underbrace{(P_{\mathrm{s}}\mathbf{V}^H(\mathbf{R}_{\mathrm{g}}^H \otimes \tilde{\mathbf{F}}\tilde{\mathbf{F}}^H)\mathbf{V})}_{\mathbf{Q}_{\mathrm{ISI}}}\mathbf{w}, \tag{27}$$

$$P_{\mathrm{LI}} = \mathbf{w}^H \underbrace{(\mathbf{V}^H(\mathbf{R}_{\mathrm{g}}^H \otimes \check{\mathbf{H}}\check{\mathbf{R}}_{\mathrm{t}}\check{\mathbf{H}}^H)\mathbf{V})}_{\mathbf{Q}_{\mathrm{LI}}} \mathbf{w}, \tag{28}$$

$$P_{\mathrm{N}} = \mathbf{w}^H \underbrace{(\sigma^2\mathbf{V}^H(\mathbf{R}_{\mathrm{g}}^H \otimes \check{\mathbf{I}}\check{\mathbf{I}}^H)\mathbf{V})}_{\mathbf{Q}_{\mathrm{N}}} \mathbf{w} + \sigma^2. \tag{29}$$

Applying (26)–(29) to the filter design methods described in Sect. 3, we can obtain the optimal filter coefficients in the partial CSI case.

5. Simulation Results

We present simulation results to evaluate the performance of the proposed FD-FF scheme. In this section, we call the two methods presented in Sects. 3.1 and 3.2 "LI Nulling" and "IPO." Unless otherwise indicated, the following simulation parameters were used: the number of relays $R = 2$; the number of relay receive antennas $N_{\mathrm{r}} = 4$; the CIR lengths $L_{\mathrm{f}} = L_{\mathrm{g}} = 10$, $L_{r,r} = 2$, and $L_{r,i(r\neq i)} = L_{\mathrm{h}} = 3$; the length of relay filter $L_{\mathrm{w}} = 10$; the decision delay $p = \lceil (L_{\mathrm{f}} + L_{\mathrm{w}} + L_{\mathrm{g}} - 2)/2 \rceil$; and the intentional delay $d = L_{\mathrm{f}} + L_{\mathrm{w}} + L_{\mathrm{g}} + 1$[†]. The modulation scheme employed was quadrature phase shift keying (QPSK). The noise power was assumed to be $\sigma^2 = 1$. Both the source transmission power P_{s} and the maximum total relay transmission power $P_{\max}$ were 10 dB higher than σ^2. We modeled the CIR path gains as zero-mean unit-variance complex Gaussian random variables with a uniform power delay profile. We conducted 10^3 simulation runs, where each run had different channels and 10^4 data symbols. We measured the actual relay transmit power $\check{P}$ by averaging over 10^4 symbols in each simulation run. For the IPO algorithm, we set the terminal tolerances of each phase $\epsilon_1 = 10^{-1}$ and $\epsilon_2 = 10^{-2}$.

First, we consider the effect of the maximum relay transmission power $P_{\max}$. Figure 2 shows the receive SINR at $\mathcal{D}$ versus $P_{\max}$. The SINR of both methods improves as $P_{\max}$ increases. Note that the performance improvement saturates because the noise in the received signal at the relays is enhanced as $P_{\max}$ increases. IPO outperforms LI Nulling, as LI Nulling reduces the degree of freedom of the filter design because of the additional constraint. In the case of the long filter length of $L_{\mathrm{w}} = 10$, the performance of LI Nulling approaches that of IPO because it has sufficient freedom.

Figure 3 shows the cumulative distribution function of the actual relay transmit power $\check{P}$. For LI Nulling, the actual power equals the maximum relay transmit power $P_{\max}$ as a result of the power constraint $P_{\mathrm{R}} = P_{\max}$. Interestingly, IPO can save the relay transmit power while maintaining better SINR performance than can LI Nulling.

Figure 4 shows the evolution of SINR with iterations of the second phase of IPO for various $P_{\max}$ and L_{w}. As expected, SINR improves as the number of iterations increases. The figure shows that SINR is maximized within five iterations. Though not shown in this figure, we observed that the first phase of IPO converged by four iterations.

Figure 5 shows SINR versus the filter length L_{w}. The performance of the conventional HD-FF scheme in [11] is also shown. As L_{w} increases, the SINR performance improves. This is because the interference suppression capability improves as L_{w} increases. We can also see that the performance of LI Nulling approaches that of IPO for suf-

[†]As far as d satisfies (10), d does not affect the performance because SINR in (12) and P_{R} in (13) do not depend on d when $t_{r,k}$ is a stationary process.

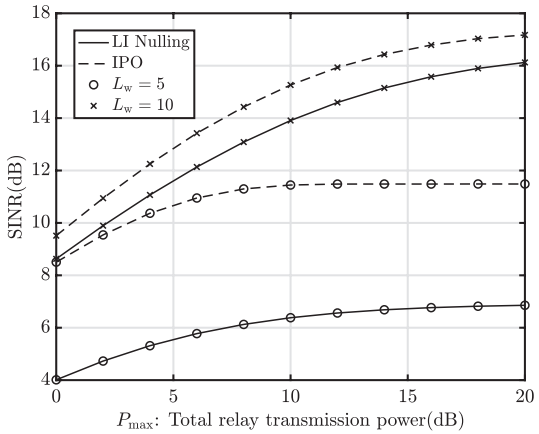

Fig. 2 Effect of relay transmission power on SINR.

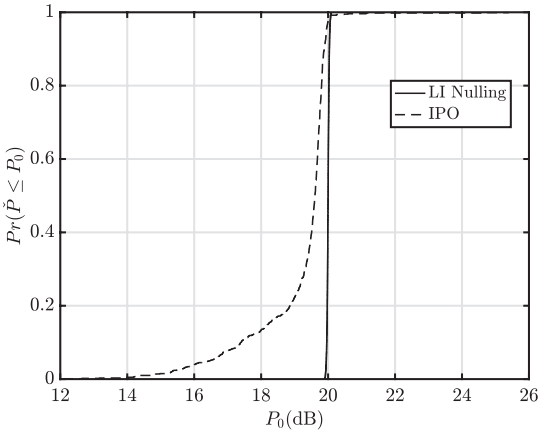

Fig. 3 CDF of the actual relay power $\check{P}$.

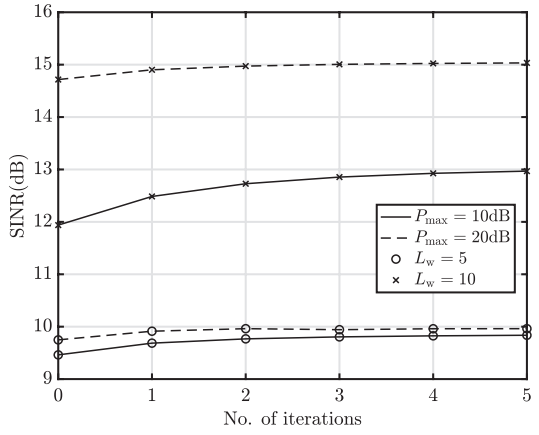

Fig. 4 Iteration characteristics of the IPO algorithm.

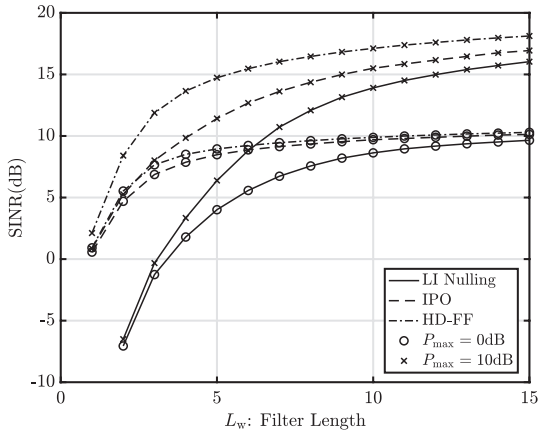

Fig. 5 Effect of filter length on SINR.

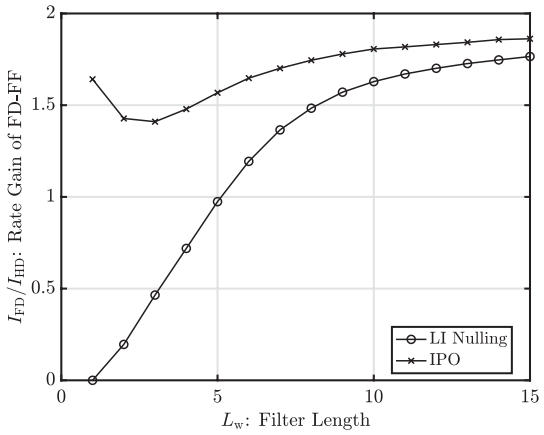

Fig. 6 Comparison of achievable rates.

ficiently large L_w. The SINR of HD-FF is higher than that of the proposed FD-FF scheme since HD-FF does not suffer from SI.

We next compare the proposed FD-FF scheme with the conventional HD-FF scheme. Figure 6 shows the achievable rate gain of the FD-FF scheme over the HD-FF scheme, I_{FD}/I_{HD}, versus L_w, where $I_{FD} \triangleq \log_2(1 + \mathrm{SINR}_{FD})$ and $I_{HD} \triangleq (1/2)\log_2(1 + \mathrm{SINR}_{HD})$. The proposed FD-FF scheme outperforms the HD-FF scheme when $L_w > 5$. For large L_w, the FD-FF scheme achieves nearly twice the performance of the HD-FF scheme.

Let us explain the behavior of the IPO curve in Fig. 6. When L_w=1, the SINR of HD-FF is poor and close to that of the FD-FF using IPO as can be seen in Fig. 5. This is because the filter length is too short to suppress interference sufficiently. Then, the resulting achievable rate of HD-FF becomes low compared to that of the FD-FF using IPO due to the effect of the coefficient 1/2 in I_{HD}. When $L_w = 2$, the SINR of HD-FF becomes better than that of the FD-FF using IPO, and the resulting achievable rate gain drops. As L_w increases further, the achievable rate gain increases since both schemes suppress interference significantly and achieve similar SINR.

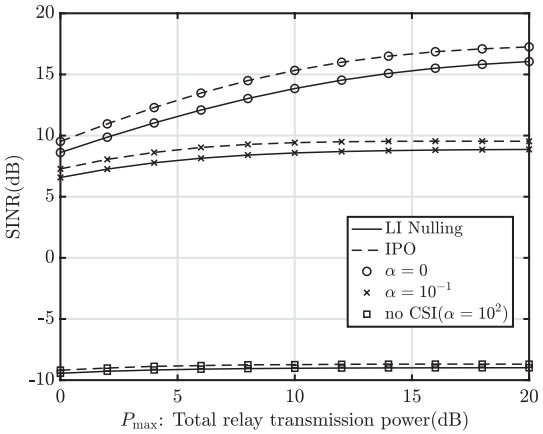

Fig. 7 Performance of SOS-based methods.

Finally, we evaluate the SOS-based design described in Sect. 4. We adopted the following model for $\mathcal{R}_r$-$\mathcal{D}$ channel path gains [14]

$$g_{r,l} \triangleq \frac{1}{\sqrt{1+\alpha}}(\bar{g}_{r,l} + \sqrt{\alpha}\tilde{g}_{r,l}) \tag{30}$$

where $\bar{g}_{r,l}$ and $\tilde{g}_{r,l} \sim \mathcal{CN}(0,1)$ are the mean and variable components of $g_{r,l}$, and the uncertainty parameter α determines the variation from its mean value. Then, the SOS of $\mathcal{R}_r$-$\mathcal{D}$ channel is given by

$$\mathbf{R}_g = \frac{1}{1+\alpha}(\bar{\mathbf{g}}\bar{\mathbf{g}}^H + \alpha \mathbf{I}_{RL_g}) \tag{31}$$

where $\bar{\mathbf{g}} \triangleq [\bar{g}_{1,0}, \cdots, \bar{g}_{R,L_g-1}]^T$. The mean value $\bar{g}_{r,l}$ was generated only once per simulation run, and 10^2 realizations of $\tilde{g}_{r,l}$ were generated for each simulation run. Figure 7 shows the performance of the SOS-based methods for various α. The case of $\alpha = 0$ corresponds to the case with full CSI. The case of $\alpha = 10^2$, which results in $\mathbf{R}_g \approx \mathbf{I}_{RL_g}$, corresponds to the case where no CSI about $\mathcal{R}_r$-$\mathcal{D}$ channels is available. We can see that the performance of the SOS-based method with $\alpha = 10^{-1}$ is worse than that of the full CSI-based method in the high P_{max} region, but is close in the low P_{max} region. Moreover, the performance of the case with $\alpha = 10^{-1}$ is significantly better than that of the case without CSI. This indicates that the SOS of CSI is useful even if the full CSI is not available.

6. Conclusion

In this paper, full-duplex relaying networks with multiple FF relays were investigated. We proposed two methods for filter design, which are based on SINR maximization with a relay transmission power constraint. Simulation results showed the effectiveness of the proposed methods, particularly when the filter was sufficiently long. We showed that the proposed FD-FF scheme outperformed the HD-FF scheme in terms of the achievable rate. In addition, SOS-based filter design methods were derived and their effectiveness was shown numerically.

To ensure that FD-FF systems are applicable to a wide variety of situations, developing filter design methods is worthwhile for cases in which individual power constraints for each relay are imposed or no central node exists.

Acknowledgments

This work was supported by JSPS KAKENHI Grant Number 17K06414.

References

[1] A. Sabharwal, P. Schniter, D. Guo, D.W. Bliss, S. Rangarajan, and R. Wichman, "In-band full-duplex wireless: Challenges and opportunities," IEEE J. Sel. Areas Commun., vol.32, no.9, pp.1637–1652, Sept. 2014.
[2] Z. Zhang, X. Chai, K. Long, A.V. Vasilakos, and L. Hanzo, "Full duplex techniques for 5G networks: Self-interference cancellation, protocol design, and relay selection," IEEE Commun. Mag., vol.53, no.5, pp.128–137, May 2015.
[3] S. Hong, J. Brand, J.I. Choi, M. Jain, J. Mehlman, S. Katti, and P. Levis, "Applications of self-interference cancellation in 5G and beyond," IEEE Commun. Mag., vol.52, no.2, pp.114–121, Feb. 2014.
[4] E. Everett, A. Sahai, and A. Sabharwal, "Passive self-interference suppression for full-duplex infrastructure nodes," IEEE Trans. Wireless Commun., vol.13, no.2, pp.680–694, Feb. 2014.
[5] J.H. Lee, J.W. Choi, J.H. Jung, S.C. Kim, and Y.H. Kim, "Analog cancellation for full-duplex wireless in multipath self-interference channels," IEICE Trans. Commun., vol.E98-B, no.4, pp.646–652, April 2015.
[6] T. Riihonen, S. Werner, and R. Wichman, "Mitigation of loopback self-interference in full-duplex MIMO relays," IEEE Trans. Signal Process., vol.59, no.12, pp.5983–5993, Dec. 2011.
[7] J.S. Lemos, F.A. Monteiro, I. Sousa, and A. Rodrigues, "Full-duplex relaying in MIMO-OFDM frequency-selective channels with optimal adaptive filtering," Proc. IEEE GlobalSIP, pp.1081–1085, Dec. 2015.
[8] M.A. Ahmed, C.C. Tsimenidis, and A.F.A. Rawi, "Performance analysis of full-duplex-MRC-MIMO with self-interference cancellation using null-space-projection," IEEE Trans. Signal Process., vol.64, no.12, pp.3093–3105, June 2016.
[9] B. Chun and H. Park, "A spatial-domain joint-nulling method of self-interference in full-duplex relays," IEEE Commun. Lett., vol.16, no.4, pp.436–438, April 2012.
[10] K. Hayashi, M. Kaneko, M. Noguchi, and H. Sakai, "A single frequency full-duplex radio relay station for frequency domain equalization systems," Proc. IEEE/CIC ICCC, pp.33–38, Aug. 2013.
[11] H. Chen, A.B. Gershman, and S. Shahbazpanahi, "Filter-and-forward distributed beamforming for relay networks in frequency selective fading channels," IEEE Trans. Signal Process., vol.58, no.3, pp.1251–1262, March 2010.
[12] Y. Liang, A. Ikhlef, W. Gerstacker, and R. Schober, "Cooperative filter-and-forward beamforming for frequency-selective channels with equalization," IEEE Trans. Wireless Commun., vol.10, no.1, pp.228–239, Jan. 2011.
[13] E. Antonio-Rodríguez, R. López-Valcarce, T. Riihonen, S. Werner, and R. Wichman, "Autocorrelation-based adaptation rule for feedback equalization in wideband full-duplex amplify-and-forward MIMO relays," Proc. IEEE ICASSP, pp.4968–4972, May 2013.
[14] V. Havary-Nassab, S. Shahbazpanahi, A. Grami, and Z.Q. Luo, "Distributed beamforming for relay networks based on second-order statistics of the channel state information," IEEE Trans. Signal Process., vol.56, no.9, pp.4306–4316, Sept. 2008.
[15] N. Bornhorst and M. Pesavento, "Filter-and-forward beamforming with adaptive decoding delays in asynchronous multi-user relay networks," Signal Process., vol.109, pp.132–147, 2015.
[16] M.M. Abdallah and H.C. Papadopoulos, "Beamforming algorithms for information relaying in wireless sensor networks," IEEE Trans. Signal Process., vol.56, no.10, pp.4772–4784, Oct. 2008.
[17] G. Liu, F.R. Yu, H. Ji, V.C.M. Leung, and X. Li, "In-band full-duplex relaying: A survey, research issues and challenges," IEEE Commun. Surveys Tuts., vol.17, no.2, pp.500–524, Secondquarter 2015.
[18] W.H. Press, S.A. Teukolsky, W.T. Vetterling, and B.P. Flannery, Numerical Recipes in C, Cambridge University Press, 1992.

Appendix: Derivation of (3) and (5)

Note that some variables used below have been defined in Sect. 2. We rewrite $\mathbf{r}_{r,k}$ in (1) as

$$\mathbf{r}_{r,k} = \mathbf{F}_r \check{\mathbf{s}}_k + \sum_{i=1}^{R} \mathbf{H}_{r,i} \check{\mathbf{t}}_{i,k} + \mathbf{n}_{r,k} \tag{A·1}$$

where $\check{\mathbf{s}}_r \triangleq [s_k \ \cdots \ s_{k-L_\mathrm{f}+1}]^T$, $\check{\mathbf{t}}_{i,k} \triangleq [t_{i,k} \ \cdots \ t_{i,k-L_\mathrm{h}+1}]^T$. We also rewrite $t_{r,k}$ in (2) as

$$t_{r,k} = \mathbf{w}_r^H \check{\mathbf{r}}_{r,k-d} \tag{A·2}$$

where $\check{\mathbf{r}}_{r,k} \triangleq [\mathbf{r}_{r,k}^T \ \cdots \ \mathbf{r}_{r,k-L_\mathrm{w}+1}^T]^T$ and it can be expressed using (A·1) as

$$\check{\mathbf{r}}_{r,k} = \begin{bmatrix} \mathbf{F}_r \check{\mathbf{s}}_k \\ \vdots \\ \mathbf{F}_r \check{\mathbf{s}}_{k-L_\mathrm{w}+1} \end{bmatrix} + \sum_{i=1}^{R} \begin{bmatrix} \mathbf{H}_{r,i} \check{\mathbf{t}}_{i,k} \\ \vdots \\ \mathbf{H}_{r,i} \check{\mathbf{t}}_{i,k-L_\mathrm{w}+1} \end{bmatrix} + \bar{\mathbf{n}}_{r,k}. \tag{A·3}$$

The first term on the right-hand side of (A·3) can be written as

$$\begin{bmatrix} \mathbf{F}_r \check{\mathbf{s}}_k \\ \vdots \\ \mathbf{F}_r \check{\mathbf{s}}_{k-L_\mathrm{w}+1} \end{bmatrix} = \bar{\mathbf{F}}_r \bar{\mathbf{s}}_k \tag{A·4}$$

where $\bar{\mathbf{F}}_r = \mathrm{toeplitz}(\mathbf{F}_r, L_\mathrm{w})$, i.e.,

$$\bar{\mathbf{F}}_r = \begin{bmatrix} \mathbf{f}_{r,0} & \cdots & \mathbf{f}_{r,L_\mathrm{f}-1} & & \mathbf{0} \\ & \ddots & & \ddots & \\ \mathbf{0} & & \mathbf{f}_{r,0} & \cdots & \mathbf{f}_{r,L_\mathrm{f}-1} \end{bmatrix}.$$

Similarly, the second term of (A·3) can be written as

$$\sum_{i=1}^{R} \begin{bmatrix} \mathbf{H}_{r,i} \check{\mathbf{t}}_{i,k} \\ \vdots \\ \mathbf{H}_{r,i} \check{\mathbf{t}}_{i,k-L_\mathrm{w}+1} \end{bmatrix} = \sum_{i=1}^{R} \bar{\mathbf{H}}_{r,i} \bar{\mathbf{t}}_{i,k} = \bar{\mathbf{H}}_r \bar{\mathbf{t}}_k \tag{A·5}$$

By substituting (A·4) and (A·5) into (A·3) and the resulting equation into (A·2), we obtain (3).

We rewrite y_k in (4) as

$$y_k = \sum_{r=1}^{R} \mathbf{g}_r^T \mathbf{t}_{r,k} + v_k \tag{A·6}$$

where $\mathbf{t}_{r,k} \triangleq [t_{r,k} \ \cdots \ t_{r,k-L_\mathrm{g}+1}]^T$. From (3), we have

$$\mathbf{t}_{r,k} = \breve{\mathbf{W}}_r^H \left\{ \begin{bmatrix} \bar{\mathbf{F}}_r \bar{\mathbf{s}}_{k-d} \\ \vdots \\ \bar{\mathbf{F}}_r \bar{\mathbf{s}}_{k-L_g+1-d} \end{bmatrix} + \begin{bmatrix} \bar{\mathbf{H}}_r \bar{\mathbf{t}}_{k-d} \\ \vdots \\ \bar{\mathbf{H}}_r \bar{\mathbf{t}}_{k-L_g+1-d} \end{bmatrix} + \begin{bmatrix} \bar{\mathbf{n}}_{r,k-d} \\ \vdots \\ \bar{\mathbf{n}}_{r,k-L_g+1-d} \end{bmatrix} \right\} \quad (A \cdot 7)$$

Since each term in the braces can be rewritten in a similar way as (A· 4) and (A· 5), we have

$$\mathbf{t}_{r,k} = \breve{\mathbf{W}}_r^H (\breve{\mathbf{F}}_r \breve{\mathbf{s}}_{k-d} + \breve{\mathbf{H}}_r \breve{\mathbf{t}}_{k-d} + \bar{\mathbf{I}} \breve{\mathbf{n}}_{r,k-d}) \quad (A \cdot 8)$$

By substituting (A· 8) into (A· 6), we have (5).

Shogo Koyanagi received the B.Eng. and M.Eng. degrees in electrical and electronic engineering from Ibaraki University, Hitachi, Japan in 2016 and 2018, respectively. In 2018, he joined Pioneer Corp., Kawagoe, Japan. His research interests include signal processing for wireless communications.

Teruyuki Miyajima received the B.Eng., M.Eng., and Ph.D. degrees in electrical engineering from Saitama University, Saitama, Japan, in 1989, 1991, and 1994, respectively. In 1994, he joined Ibaraki University, Hitachi, Japan, where he is currently a professor. His current interests are in signal processing for wireless communications. Dr. Miyajima is a member of IEEE.